THE JOURNAL OF PHYSICAL CHEMISTRY B

Article

pubs.acs.org/JPCB

Intramolecular Electronic Couplings in Class II/III Organic Mixed-Valence Systems of Bis(1,4-dimethoxybenzene)

Juanhua Yang, Weiwei Zhang, Yubing Si, and Yi Zhao*

State Key Laboratory of Physical Chemistry of Solid Surfaces, Fujian Provincial Key Lab of Theoretical and Computational Chemistry, and College of Chemistry and Chemical Engineering, Xiamen University, Xiamen 361005, P. R. China

Supporting Information

ABSTRACT: The intramolecular electronic couplings in organic mixed-valence systems $[D\text{-}(ph)_n\text{-}D]^{\bullet+}$ (D = 2,5-dimethoxy-4-methylphenyl, n = 0, 1, and 2) are calculated by dominantly using density functional theory to investigate their dependence of functionals. Since these systems have the property that the charge is from localization to delocalization, the optimized structures are sensitive to the functionals. The geometric optimizations show that CAM-B3LYP and ωB97X-D functionals are good choices for delocalized systems and LC-ωPBE and M06HF are suitable for the systems from charge almost localization to localization. The calculations of electronic couplings demonstrate that the pure functional generally underestimates the electronic couplings whereas the pure HF overestimates them. Furthermore, the electronic couplings from the conventional generalized Mulliken-Hush method are very sensitive to the HF component in functionals, which makes it a challenge to accurately estimate the values. A new reduced two-state method is thus proposed to overcome the deficiency, and the obtained electronic couplings are less sensitive to the ω value in LC-ω PBE functional and they are also consistent with the experimental data.

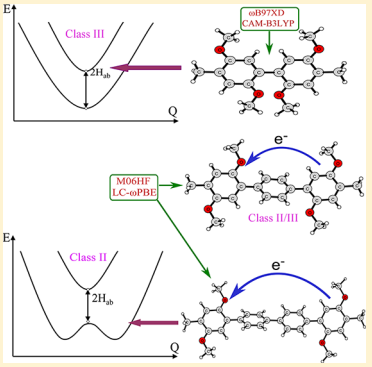

1. INTRODUCTION

Organic mixed-valence (MV) systems are commonly composed of two or more redox centers connected by either saturated or unsaturated bridges. They have attracted a broad attention in the investigation of electron transfer (ET) due to their charge distributions covering from localization to delocalization.[1−9] According to the strength of electronic coupling between donor and acceptor states, Robin and Day divided MV systems into three classes.[10] Class I refers to the systems in which the electronic couplings are zero and no ET occurs. Class II includes the charge-localized systems with weak electronic couplings, and the charge can transfer from one redox center to the other. Class III corresponds to those with strong electronic couplings, and the charge is essentially delocalized. Since then, different kinds of redox centers of MV systems have been proposed, such as diquinone,[11,12] diketone,[13] pyridinium,[14] hydrazines,[15−23] triarylamines,[24−31] and bis(alkoxy)-benzene.[32−38] Recently, it was found that many MV systems are borderline between classes II and III, where the charge is almost delocalized. This property makes it a challenge to investigate intramolecular ET in those systems from both experiments and theories.[35,39−43]

Theoretically, ET rate is determined by three key factors, electronic coupling, reorganization energy, and driving force. Once those parameters are known, several rate theories[44−48] can be used to predict the ET rates from weak to strong electronic coupling regime. In the three factors, the reorganization energy and driving force dominantly come from the individual contributions of two redox centers, and they can be quite accurately determined by available electronic structure theories.[23,49−52] However, it is not easy to accurately calculate the electronic couplings especially for the MV systems connected with bridges because the electronic couplings essentially represent the long-range interaction between two redox centers. In this paper, we take $[D\text{-}(ph)_n\text{-}D]^{\bullet+}$ (D = 2,5-dimethoxy-4-methylphenyl, n = 0, 1, and 2) as model systems to prove the reliable approaches in practice for the calculations of electronic couplings. The $[D\text{-}(ph)_n\text{-}D]^{\bullet+}$, as shown in Figure 1, are good candidates to systematically investigate the dependence of electronic couplings on different electronic structure methods because the experimental results[35] have already demonstrated that those systems can change from one class to the other with an increase of bridges, i.e., $[D\text{-}D]^{\bullet+}$, $[D\text{-}ph\text{-}D]^{\bullet+}$, and $[D\text{-}(ph)_2\text{-}D]^{\bullet+}$ belong to classes III, II/III borderline, and II, respectively.

The available theoretical models for the calculations of electronic couplings are based on two strategies, one is starting from the adiabatic representation and the other is from the diabatic representation. The Koopmans' theorem (KT), generalized Mulliken-Hush method (GMH), and Spin-Flip model are examples in the adiabatic representation,[53−56] whereas the two-state model (TM) and reduced TM (RTM)[53,57] come from the diabatic representation. In this paper, both models from the adiabatic and diabatic representations are adopted for the purpose of comparison. Furthermore, we propose a new numerical technique, a

Received: August 19, 2012
Revised: November 12, 2012
Published: November 13, 2012

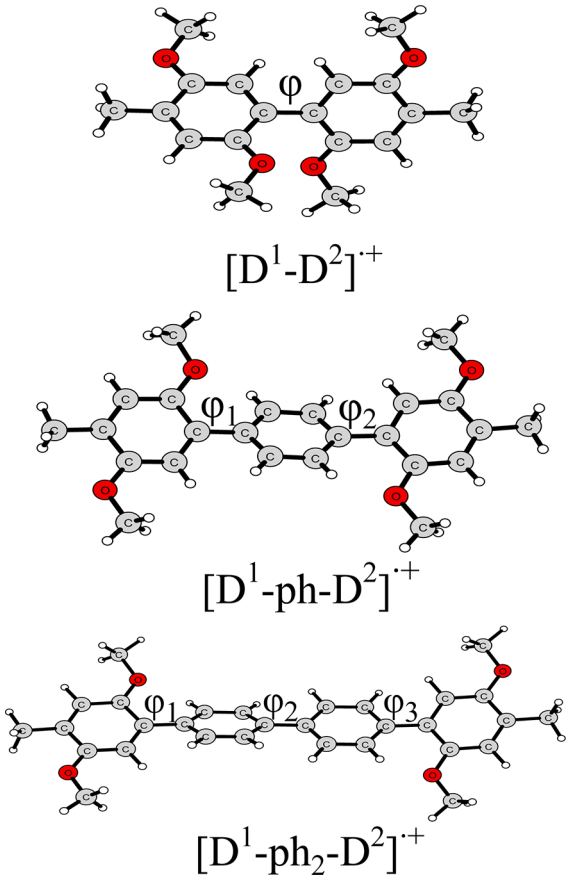

Figure 1. Structures of organic mixed-valence systems $[D\text{-}(ph)_n\text{-}D]^{\bullet+}$ (D = 2,5-dimethoxy-4-methylphenyl, n = 0, 1, and 2); the D^1 and D^2 refer to the left and right redox centers, respectively. The D^1 and D^2 have C_2 symmetry in $[D\text{-}D]^{\bullet+}$, and they show C_i symmetry in $[D\text{-}ph\text{-}D]^{\bullet+}$ and $[D\text{-}(ph)_2\text{-}D]^{\bullet+}$.

modified RTM (mRTM) in which the diabatic wave functions are constructed from adiabatic ones. The mRTM avoids splitting the systems into donor and acceptor fragments, and it is very suitable for the calculations of strong electronic couplings in intramolecular ET.

In the above models for the calculations of electronic couplings, one needs to know the electronic structure properties, such as excitation energies, dipole moments and electronic wave functions of the systems. In principle, accurate electronic structure methods should be adopted to rigorously predict those quantities. For instance, the complete active space self-consistent field or higher accurate calculations should be used. But these high accurate calculations are still limited to small systems for the moment. Alternatively, semiempirical methods, HF and MP2 approaches, density functional theory (DFT) methods, and so on,[27,58−66] have been widely applied to calculate the electronic couplings. Although they have been successfully applied to a series of MV systems, they have individual demerits. For instance, the precision of semiempirical methods is usually limited by utilizing empirical parameters,[64,67] the HF method normally overestimates charge localization for relative large organic MV systems,[39,60] and the DFT and time dependent DFT (TDDFT) with "pure" or standard hybrid exchange-correlation functionals are not accurate in the applications to the systems with long-range ET and strong polarizations. Recently, the results from Martin Kaupp group[5] have indicated that the nonstandard hybrid DFTs with 35% Hartree−Fock (HF) are appropriate for the quantum-chemical characterization of organic MV systems. In our previous works,[23,52] we have also investigated the influence of HF component on the electronic couplings and structures. However, it is still not clear to determine the percent of HF exchange for different classes of MV systems. On the other hand, several groups[68−75] have proposed the novel DFTs, especially the long-range corrected DFTs (LRC-DFTs), to calculate the electronic couplings of the organic MV systems,[64,66,76,77] and the time dependent LRC-DFTs (TD-LRC-DFTs) have been applied to accurately estimate the excitation energy.[78−80] Therefore, in the present paper, we will systematically investigate whether the novel DFTs can predict reasonable results for such kinds of systems. Concretely speaking, we will optimize geometries and calculate the electronic couplings with different electronic structure methods to find the suitable methods for classes II to III MV systems. In the calculations, we adopt HF, DFTs with a variety of LRC-DFTs (such as CAM-B3LYP, LC-ωPBE, ωB97X, and ωB97X-D), and DFTs with standard hybrid functionals (DFT/50−50, B3LYP) and global hybrid meta-GGA functional M06HF. Furthermore, the dependence of electronic couplings on the long-range correction component in LC-ωPBE is revealed by using the different values of ω.

The paper is arranged as follows: in section II, we briefly review available approaches and show a new method for the calculations of electronic couplings. Section III presents the results and discussions, and concluding remarks are given in section IV.

2. CALCULATION METHODS

2.1. Models for the Calculation of Electronic Coupling. Electronic coupling V_{DA} presents the electronic interaction between the donor and acceptor states. Several models from the diabatic and adiabatic representations have been reviewed in the recent papers.[81−83] Here, we only outline KT, GMH, and RTM methods which are concerned in this work.

In the adiabatic representation, the electronic coupling is given by half of the energy gap of two adiabatic eigenvalues at transition state (TS) geometry. In the well-known KT method, these adiabatic eigenvalues are approximated by the energies of the molecular orbitals (MOs) of the neutral system.[54,84,85] Concretely speaking, the electronic couplings of hole transfer and ET can be given by

$$V_{DA} = \frac{\varepsilon_{HOMO} - \varepsilon_{HOMO-1}}{2} \quad \text{(for hole transfer)} \tag{1}$$

and

$$V_{DA} = \frac{\varepsilon_{LUMO+1} - \varepsilon_{LUMO}}{2} \quad \text{(for ET)} \tag{2}$$

Here ε_i is the MO energy of neutral system at the TS geometry of ionic system (HOMO and LUMO represent the highest occupied MO and the lowest unoccupied MO, respectively). It is easy to determine the TS geometry for a symmetrical ET, where the driving force is zero, and the charge is symmetrically distributed on both sides of the ionic system at the TS geometry. For a unsymmetrical ET, the TS geometry cannot be straightforwardly determined. A common way to find the TS geometry is to introduce a linear reaction coordinate R[23,53,86]

$$Q_i = RQ_i^{a} + (1 - R)Q_i^{d} \tag{3}$$

dx.doi.org/10.1021/jp308242s | J. Phys. Chem. B 2012, 116, 14126−14135

where Q_i is the ith internal coordinate (bond length, bond angle, or dihedral) and d and a correspond to the donor and acceptor, respectively. Obviously, R = 0 and 1.0 refer to the optimized geometries of the donor and acceptor states, respectively. The TS geometry is thus found from eq 3 at the given R where the energy gap of MOs is minimum.

Alteratively, the GMH is generally used to estimate the electronic coupling at the optimized geometry of ionic systems[55,87−89]

$$V_{DA} = \frac{\mu_{12}\Delta E_{12}}{\sqrt{\Delta\mu_{12}^{\ 2} + 4\mu_{12}^{\ 2}}} \tag{4}$$

Here ΔE_{12} is the vertical excitation energy, μ_{12} is the transition dipole moment, and $\Delta\mu_{12}$ is the difference of dipole moment between the adiabatic donor and acceptor states.

In the diabatic representation, the electronic coupling in the TM is related to the off-diagonal elements of the Hamiltonian for ionic systems.[53,90] In the TM, one needs to obtain the wave functions of two diabatic states, Ψ_1 and Ψ_2. Defining $h_{ij} = \langle\Psi_i|H|\Psi_j\rangle$ (i, j = 1, 2) and $s_{12} = \langle\Psi_1|\Psi_2\rangle$, the electronic coupling can be calculated by the following expression:

$$V_{DA} = \frac{h_{12} - s_{12}(h_{11} + h_{22})/2}{1 - s_{12}^{\ 2}} \tag{5}$$

and the site energies are given by

$$H_{11(22)} = \frac{(h_{11} + h_{22}) - 2h_{12}s_{12} \pm (h_{11} - h_{22})\sqrt{1 - s_{12}^{\ 2}}}{2(1 - s_{12}^{\ 2})} \tag{6}$$

However, the diabatic states are not uniquely defined from given adiabatic states. The TM based on "symmetry broken" self-consistent field (SCF) states was introduced and extensively applied by Newton et al. and Larsson et al.[91−96] and reviewed by Newton et al.[87,88,97] This approach was adopted by Dupuis et al.[53,98] In the realistic applications of this TM, it is uneasy to construct the diabatic wave functions for the MV systems with strong electronic couplings. To overcome this difficulty, Brédas et al.[57] have proposed an easy way to obtain the diabatic states for "intermolecular" ET. In the approach, they use the wave functions of HOMO or LUMO of two fragment neutral monomers for hole or electron transfer to replace those of two diabatic states. The mechanism is based on the KT mechanism, and the Fock matrix and wave functions of MOs are thus corresponding to the neutral systems at the ionic geometry. We name this simplified method as RTM. In the RTM, the MOs only from the HF SCF calculations have an appropriate physical criterion. Interestingly, many practical DFT calculations reveal that the energies and wave functions of the MOs are quite accurate. For instance, Brédas et al.[57] have manipulated the RTM in the DFT scheme. In the present work, we use both of the DFT and HF SCF calculations to get the Fock/Kohn−Sham matrix for the purpose of comparison. For the systems involved in intramolecular ET, however, it is not clear how to divide systems into two fragments to define the localized diabatic wave functions. Fortunately, we find that the combinations of the adiabatic MO wave functions from the ionic system have localized properties. For instance, the HOMO and SOMO (singly occupied molecular orbital) for class II ionic systems themselves in the Franck−Condon regime are essentially localized (The TDDFT calculation indicates that the ET in the ionic system corresponds to the electronic excitation from HOMO to SOMO, thus both MOs are concerned.), and the subtraction and addition of the MO wave functions are localized at the TS geometry (the diabatic energy crossing point). Based on this observation, for the systems belonging to the borderline class II/III, we introduce a parameter ξ, similar to the linear reaction coordinate R in eq 3, to define the two new diabatic wave functions

$$\Phi_1 = \frac{1}{\sqrt{1 + \xi^2}}(\xi\phi_{SOMO} + \phi_{HOMO}) \tag{7}$$

and

$$\Phi_2 = \frac{1}{\sqrt{1 + \xi^2}}(\phi_{SOMO} - \xi\phi_{HOMO}) \tag{8}$$

Here ξ is in the range from 0 to 1, i.e., ξ = 0 and 1 for the localized and delocalized systems, respectively. The present method is named as mRTM because it is still based on the KT mechanism, similar to the RTM except the choices of diabatic wave functions. It should be addressed that these new wave functions must satisfy the condition of the TM. For instance, the energies of two diabatic states (H_{11} and H_{22} in eq 6) should be equal at the TS geometry (the energy crossing point). We will show in the next section that the new diabatic wave functions indeed satisfy this condition and they are even better than those proposed by Brédas et al.

2.2. Electronic Structure Methods. We optimize the geometries and calculate the electronic couplings by a variety of DFTs dominantly including LRC-DFTs. The detailed descriptions of the related functionals are as follows. In the conventional hybrid exchange-correlation functionals, B3LYP contains 20% HF + 80% Slater local + 72% Becke 88 nonlocal exchanges and 19% VMN local + 81% LYP nonlocal correlations.[99,100] DFT/50−50 is composed of 50% HF + 8% Slater + 42% Becke for exchange and 19% VWN + 81% LYP for correlation functionals.[101] Global hybrid meta-generalized gradient approximation(GGA) functional M06HF comprises full HF exchange and hence eliminates self-exchange interaction at long-range.[70,71] In the LRC-DFTs proposed recently, CAM-B3LYP consists of 65% HF + 35% Becke 1988(B88) long-range exchange and 19% HF + 81% B88 short-range exchange and 0.19% VWN5 + 0.81% LYP correlation.[68] Another alternative category LRC-DFTs are widely used by incorporating 100% HF exchange at long-range, whereas the traditional functionals is adopted in short-range. For this kind of LRC-DFTs, ω is introduced to determine the length scale over which the long-range is turned on, for example, ω = 0, the long-range is zero and it becomes conventional DFT.[72,102,103] Three LRC-DFTs are used in present works, they are LC-ωPBE(C_{HF} = 0.0), ωB97X(ω = 0.3a_0^{-1}, C_{HF} = 0.157706) and ω B97X-D (ω = 0.2a_0^{-1} and C_{HF} = 0.222 with damped dispersion correction). LC-ωPBE is a long-range-corrected GGA exchange-correlation functional, whose short-range part is ωPBE[69,73,74,103] (the default value of ω is 0.4 in Gaussian 09). ωB97X and ωB97X-D are two hybrid exchange-correlation functionals, which include a fraction (C_{HF} × 100%) of HF exchange in the short-range part.[75,102,104−106] The geometric optimizations with use of the standard hybrid exchange-correlation functionals and HF method are manipulated in the Gaussian 09 suite.[107] Q-Chem program[108] is employed for LC-DFTs calculations. The 6-31G(d,p) basis set is adopted in all calculations.

3. RESULTS AND DISCUSSION

3.1. Optimized Geometries. We first consider the system $[D\text{-}D]^{\bullet+}$. The HF and DFT methods are first used to optimize its geometry. Natural population analysis (NPA) is then made for the two different redox centers D^1 and D^2. It is found that $[D\text{-}D]^{\bullet+}$ shows an approximate C_2 symmetry. The corresponding results of theoretical structural parameters and charge populations, as well as those from the experiment, are listed in Table S1 of the Supporting Information (SI). For this system, the experiment[35] has demonstrated that the charge equally locates on D^1 and D^2, and it is thus classified to class III. Theoretically, the standard hybrid functionals B3LYP and DFT/50−50, as well as HF, can correctly predict such charge distributions. However, through insight into the geometrical parameters of two redox centers, it is found that the results of B3LYP are closer to the experimental data while DFT/50−50 and HF predict the shorter bond lengths, showing that a large percent of HF exchange leads to a large deviation of the structure. In the methods of LRC-DFTs and global hybrid meta-GGA, ωB97X-D and CAM-B3LYP can produce correct charge distributions, whereas ωB97X, LC-ωPBE, and M06HF predict almost localized (class II/III) character and the predicted bond lengths are clearly different from the experimental results for D^1 and D^2. In order to further confirm the validity of ωB97X-D, CAM-B3LYP, and B3LYP, we have compared the twisting angles between two benzene rings and the central C(Ar)-C(Ar) bond lengths with the experimental results (shown in Table S2). It is found that ωB97X-D and CAM-B3LYP predict closer values to the experimental data. However, the twisting angle obtained from B3LYP is much larger than the experimental one. Therefore, it may be a good choice to use LRC-DFTs with ωB97X-D and CAM-B3LYP to predict the geometry of MV system $[D\text{-}D]^{\cdot+}$ with delocalized charge distribution.

For the systems $[D\text{-ph-}D]^{\bullet+}$ and $[D\text{-}(ph)_2\text{-}D]^{\bullet+}$, their D^1 and D^2 are connected by the phenyl ring bridges through C−C single bonds, which may rotate and lead to several isomer structures. Therefore, in order to compare with the experimental results, one has to pay attention to finding out the reasonable geometries in the optimization calculations. Our investigations show that the predicted twisting angles with all of the present electronic structure methods are generally larger than the experimental ones. This is not surprising because the experimental values are measured from the crystal structures while the present results are obtained from the calculations of single molecules in the gas phase. In order to find out how the charge distributions are affected by the twisting angles, we further optimize the geometries with the twisting angles fixed to the values of experiment,[35] in which the measured angles (see in Figure 1) are $\varphi_1 = 32.0°$, $\varphi_2 = -28.6°$ for $[D\text{-ph-}D]^{\bullet+}$ and $\varphi_1 = 36.4°(Ar(D^1)\text{-}Ar(bridge_1))$, $\varphi_2 = -16.9°$, $\varphi_3 = -31.4°$ for $[D\text{-}(ph)_2\text{-}D]^{\bullet+}$, respectively. Tables S3−S4 display examples for the charge distributions and bond lengths obtained from M06HF and LC-ωPBE with and without fixed angles. It is interesting to find that the charge distributions from the constrained optimization calculations are nearly the same as those from the full optimizations, furthermore, the bond lengths are also nearly the same. It indicates that slightly different twisting angles do not affect the localized properties. However, the twisting angles may have an obvious influence for the electronic couplings. Therefore, in order to compare the theoretical results with the experimental ones at the same level, we fix the twisting angles at the experimental values in both the geometrical optimizations and electronic coupling calculations.

At the given twisting angles, the optimized geometric parameters are shown in Table S5. It is found that $[D\text{-ph-}D]^{\bullet+}$ and $[D\text{-}(ph)_2\text{-}D]^{\bullet+}$ are close to C_i symmetry. The results further indicate that B3LYP and ωB97X-D predict delocalization charge properties for $[D\text{-ph-}D]^{\bullet+}$, and ωB97X gives out 70% localized charge. Compared with the experimental one (80%),[35] all of them fail to predict the reasonable charge populations. However, about 80% charges obtained from HF, M06HF, and LC-ωPBE are in agreement with experimental one very well. Furthermore, from the bond lengths, especially δ bond lengths used to determine the charge distribution experimentally[35] (see in Figure 2), we find that DFTs with

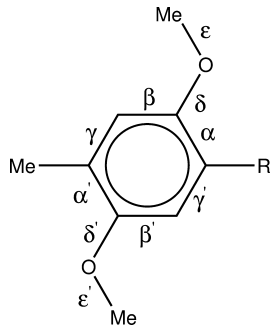

Figure 2. Structure of redox center D.

M06HF and LC-ωPBE predict the consistent results compared to the experiments whereas the HF produces the shorter δ bond length. Therefore, M06HF and LC-ωPBE may be the reasonable functionals to optimize the geometries of $[D\text{-ph-}D]^{\bullet+}$ with partially localized charge (the class II/III). For the charge fully localized system $[D\text{-}(ph)_2\text{-}D]^{\bullet+}$, one expects that DFTs with M06HF and LC-ωPBE should also be suitable in the optimization calculations from the above analysis. Indeed, the predicted charge distributions and geometries with them are consistent with the experimental results, as shown in Table S6. In addition, we also find that the spin contaminations in those systems are very small, as listed in Table S7. This allows us to use the TM to estimate electronic couplings.

In summary, Table 1 lists the suitable electronic structure methods for the optimization calculations of systems $[D\text{-}(ph)_n\text{-}D]^{\bullet+}$ (n = 0, 1 and 2) and the corresponding charge distributions, as well as the results of the experiments. The geometric parameters are labeled in Figure 2.

3.2. Electronic Coupling Calculations. Both experimental measurements and theoretical calculations have shown that the charges of the present MV systems cover from the full delocalization for $[D\text{-}D]^{\bullet+}$ to localization for $[D\text{-}(ph)_2\text{-}D]^{\bullet+}$. Therefore, these systems are good candidates to investigate which electronic structure methods for geometric optimizations and the calculation of electronic coupling are suitable for the MV systems.

For the system $[D\text{-}D]^{\bullet+}$ with delocalized charge distribution, its optimized geometry corresponds to the crossing point of two diabatic potentials because of the symmetric ET. Therefore, the KT can be straightforwardly used to evaluate the electronic couplings at the optimized geometries. Table 2 lists the electronic couplings from the KT at the optimized geometries obtained from LRC-DFTs with ωB97X-D and CAM-B3LYP. For the purpose of comparison, different

Table 1. Comparison of X-ray Results and Optimized Geometric Parameters for the Redox Centers of the MV Systems $[D\text{-}(ph)_n\text{-}D]^{\bullet+}$ (n = 0, 1, and 2)[a]

systems	methods	L	α/α'	β/β'	γ/γ'	δ/δ'	ε/ε'	q_i[b]
$[D\text{-}D]^{\bullet+}$	ωB97X-D	D^1	1.430/1.431	1.404/1.383	1.379/1.405	1.329/1.338	1.423/1.420	+0.5
		D^2	1.430/1.431	1.404/1.383	1.379/1.405	1.329/1.338	1.423/1.420	+0.5
	CAM-B3LYP	D^1	1.429/1.429	1.402/1.382	1.378/1.404	1.331/1.340	1.425/1.421	+0.5
		D^2	1.429/1.429	1.402/1.382	1.378/1.404	1.331/1.340	1.425/1.421	+0.5
	X-ray	D^1	1.444/1.432	1.400/1.377	1.378/1.408	1.341/1.356	1.435/1.442	+0.5
		D^2	1.442/1.420	1.402/1.383	1.379/1.410	1.344/1.356	1.452/1.442	+0.5
$[D\text{-}ph\text{-}D]^{\bullet+}$	LC-ωPBE	D^1	1.447/1.441	1.408/1.388	1.367/1.391	1.314/1.320	1.429/1.426	+0.77
		D^2	1.401/1.402	1.395/1.381	1.382/1.403	1.358/1.357	1.412/1.407	+0.09
	M06HF	D^1	1.451/1.445	1.424/1.406	1.364/1.382	1.304/1.310	1.438/1.435	+0.83
		D^2	1.401/1.404	1.400/1.386	1.386/1.405	1.361/1.358	1.418/1.414	+0.06
	X-ray	D^1	1.440/1.436	1.411/1.387	1.377/1.397	1.331/1.344	1.449/1.444	+0.8
		D^2	1.416/1.410	1.399/1.383	1.393/1.409	1.363/1.369	1.432/1.435	+0.2
$[D\text{-}(ph)_2\text{-}D]^{\bullet+}$	LC-ωPBE	D^1	1.447/1.441	1.409/1.394	1.366/1.384	1.311/1.317	1.430/1.428	+0.82
		D^2	1.399/1.398	1.394/1.383	1.384/1.400	1.362/1.360	1.409/1.406	+0.04
	M06HF	D^1	1.449/1.445	1.424/1.411	1.364/1.377	1.303/1.308	1.438/1.437	+0.86
		D^2	1.401/1.401	1.399/1.388	1.387/1.403	1.363/1.361	1.416/1.413	+0.03
	X-ray	D^1	1.446/1.435	1.411/1.401	1.371/1.383	1.325/1.324	1.454/1.448	+1.0
		D^2	1.410/1.396	1.392/1.392	1.393/1.410	1.370/1.385	1.440/1.419	0.0

[a]Units for bond lengths are Angstrom. [b]Charge is estimated from NPA.

Table 2. Calculated Electronic Coupling (cm^{-1}) for the $[D\text{-}D]^{\bullet+}$[a]

geometries[b]	methods[c]	KT	GMH	RTM	mRTM	ΔE(RTM)[d]	ΔE(mRTM)[d]
ωB97X-D	ωB97X-D	2332	2516	2124	1960	3.8×10^{-5}	0.48×10^{-5}
	CAM-B3LYP	2305	2642	2114	2004	3.5×10^{-5}	0.12×10^{-5}
	DFT/50−50	2524	2744	2337	2299	3.8×10^{-5}	0.11×10^{-5}
	B3LYP	1943	3136	1826	1782	3.2×10^{-5}	0.31×10^{-5}
	HF	3434	5201	3151	3167	4.6×10^{-5}	0.53×10^{-5}
CAM-B3LYP	ωB97X-D	2315	2502	2128	1985	0.42×10^{-5}	0.14×10^{-5}
	CAM-B3LYP	2292	2629	2098	2020	0.51×10^{-5}	0.19×10^{-5}
	DFT/50−50	2509	2730	2323	2309	0.49×10^{-5}	0.11×10^{-5}
	B3LYP	1926	3119	1851	1787	0.47×10^{-5}	0.23×10^{-5}
	HF	3423	5183	3140	3182	1.2×10^{-5}	2.3×10^{-5}

[a]The experimental electronic coupling is 2300 cm^{-1} from ref 35. [b]The functionals used for the geometric optimization. [c]The methods for the calculation of electronic coupling. [d]The unit of ΔE is a.u..

electronic structure methods are used in the calculations of the energies of HOMO and HOMO-1. It is found that the electronic couplings predicted from ωB97X-D and CAM-B3LYP are extremely consistent with the experimental one. However, both HF and DFT/50−50 with higher percent of HF exchange overestimate the electronic couplings while B3LYP underestimates it. In the GMH, we need to calculate the vertical excitation energy, transition dipole moment between two adiabatic states and dipole moment difference of these two states. For the charge-delocalized systems with symmetric ET, we note that two diabatic states are strongly mixed together to construct the adiabatic states. Therefore, the dipole moments in two adiabatic states and their difference may become very small even though they might be large in the diabatic states. The present calculations indeed show the very small difference dipole moments. As a result, the electronic coupling with GMH is determined by the vertical excitation energy and the obtained results are also listed in Table 2.

It shows that the electronic couplings dependence of different electronic structure methods from the GMH have a similar trend to those from the KT, but their values are always larger than those of KT and experimental result. It also shows that the accuracy of vertical excitation energy calculations between two adiabatic states need to be further improved when the GHM is used. On the other hand, our tests show that the conventional TM model in diabatic representation is not easy to manipulate because it is difficult to define the two diabatic wave functions at the optimized geometries of $[D\text{-}D]^{\bullet+}$. Fortunately, the RTM proposed by Brédas et al.[57] can be applied to this system and the obtained results are basically consistent with those of KT and GMH, as shown in Table 2. Since the electronic coupling of the present system is accurately predicted theoretically, we can demonstrate the accuracy of mRTM proposed by us. The numerical implementation is similar to RTM, except that the diabatic wave functions are obtained from eqs 7 and 8, and ξ is chosen to be 1 due to the fully delocalized properties of wave functions for both HOMO and SOMO in beta spin. Figure 3 displays the wave functions of HOMO and SOMO and their combinations at the optimized geometry obtained with ωB97X-D. Indeed, their combinations have charge localized properties. The values of electronic couplings with the mRTM are also listed in Table 2. We find that the electronic couplings calculated from the mRTM are very close to the values from RTM. The reason of slight difference can be further analyzed from the energy gaps ($\Delta E = H_{11} - H_{22}$) of the two diabatic states shown in Table 2. It

dx.doi.org/10.1021/jp308242s | J. Phys. Chem. B 2012, 116, 14126−14135

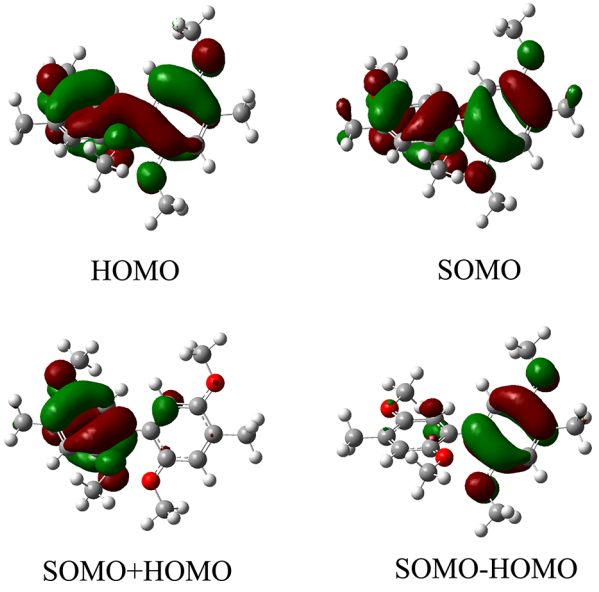

Figure 3. MOs of beta spin electron and their combinations for the radical cation $[D\text{-}D]^{\bullet+}$ at the optimized geometry with ωB97X-D.

clearly shows that the energy gaps from the mRTM are very small. This result manifests that the new wave functions satisfy the condition of TM and they are even better than those from RTM (see in Table 2). Comparing with the experimental geometries and electronic couplings, we conclude that LRC-DFTs with ωB97X-D and CAM-B3LYP together with the KT, GMH, RTM, and mRTM models may be suitable to obtain both the optimized geometries and electronic couplings for the class III MV systems.

As the benzene rings are added to the system $[D\text{-}D]^{\bullet+}$, the charge may hop from one redox center to the bridge, succeedingly to the other redox center, or transfer directly between two redox centers by tunneling. Here, we only focus on the electronic couplings for the tunneling, which is very interesting in the investigation of long-range charge transfer. The experiment[35] shows that the charge distributions are partially and fully localized for $[D\text{-ph-}D]^{\bullet+}$ and $[D\text{-}(ph)_2\text{-}D]^{\bullet+}$, respectively. So the KT cannot be straightforwardly applied to calculate the electronic coupling because the optimized geometries are not the crossing points of two diabatic potentials. The GMH and RTM models may be better choices for class II and class II/III MV systems.

Tables 3 and 4 list the electronic couplings from the GMH and mRTM models for MV systems $[D\text{-ph-}D]^{\bullet+}$ and $[D\text{-}(ph)_2\text{-}D]^{\bullet+}$ at the optimized geometries obtained from M06HF and LC-ωPBE, respectively. The results from the GMH are performed using the Q-Chem software. Before comparing the calculated results with the measured ones, we should mention that the values of experimental electronic coupling of $[D\text{-ph-}D]^{\bullet+}$ are quite different. For instance, they are 760, 1600, and 2400 cm^{-1} determined from Mulliken-Hush method, cyclic voltammetry (CV) method and X-ray crystallography, respectively.[34,35] We think that 1600 cm^{-1} should be a good one because this system belongs to the class II/III border,[35] and its electronic coupling should be between 2330 ($[D\text{-}D]^{\bullet+}$) and 430 cm^{-1} ($[D\text{-}(ph)_2\text{-}D]^{\bullet+}$) and close to 2330 cm^{-1}. The tables show that B3LYP and DFT/50−50 underestimate the electronic couplings for both MV systems, but the HF method overestimates them. Moreover, it seems that the LC-ωPBE for $[D\text{-ph-}D]^{\bullet+}$ and both LC-ωPBE and M06HF for $[D\text{-}(ph)_2\text{-}D]^{\bullet+}$ are suitable to predict the reasonable electronic couplings compared to the experimental ones. As M06HF has a large component of HF exchange, it is very suitable for the charge localized systems. Indeed, the experimental charge in $[D\text{-}(ph)_2\text{-}D]^{\bullet+}$ is nearly localized to be 1, whereas $[D\text{-ph-}D]^{\bullet+}$ has about 0.8 localized charge; thus, LC-ωPBE should be a good choice to describe the two kinds of MV systems. It is noted that our previous works[23,52] have confirmed that DFT/50−50 is a reasonable functional for the systems with 0.8 localized charge, but it predicts too small electronic coupling for $[D\text{-ph-}D]^{\bullet+}$. The reason may be that the redox centers in the present system are connected by an unsaturated bridge compared to the previous systems, as a results, the long-range interaction becomes more important. From the calculated results of optimized geometries and electronic couplings, we thus propose that LC-ωPBE is appropriate for the investigation of systems with both partially (0.7−0.8) and fully localized charge,

Table 3. Calculated Electronic Coupling (cm^{-1}) for $[D\text{-ph-}D]^{\bullet+}$[a]

geometries[b]	methods[c]	GMH	mRTM-1	mRTM-2	mRTM-3
LC-ωPBE	CAM-B3LYP		129	1129	1004(ξ = 0.2)
	ωB97X-D		590	1145	1018(ξ = 0.1)
	B3LYP	513	1013	984	1748(ξ = 0.9)
	DFT/50−50	669	51	1202	1367(ξ = 0.3)
	ωB97X	559	1032	1162	1032(ξ = 0)
	LC-ωPBE	1223	1150	1150	1150(ξ = 0)
	M06HF	3221	1383	1278	1383(ξ = 0)
	HF-CIS	3960	3227	1498	3227(ξ = 0)
M06HF	CAM-B3LYP		101	1009	1060(ξ = 0.2)
	ωB97X-D		543	1020	1448(ξ = 0.2)
	B3LYP	724	1337	864	1746(ξ = 0.9)
	DFT/50−50	496	3	1114	1498(ξ = 0.3)
	ωB97X	1015	893	1118	893(ξ = 0)
	LC-ωPBE	1352	965	1012	965(ξ = 0)
	M06HF	1899	1202	1202	1202(ξ = 0)
	HF-CIS	5138	2750	1485	2750(ξ = 0)

[a]The experimental electronic coupling is 1600 cm^{-1} from ref 35. [b]The functionals used for the geometric optimization. [c]Different electronic structure methods used to calculate the electronic coupling.

dx.doi.org/10.1021/jp308242s | J. Phys. Chem. B 2012, 116, 14126−14135

Table 4. Calculated Electronic Coupling (cm^{-1}) for $[D\text{-}(ph)_2\text{-}D]^{\bullet+}$[a]

geometries[b]	methods[c]	GMH	mRTM-1	mRTM-2	mRTM-3
LC-ωPBE	CAM-B3LYP		45	709	447 (ξ = 0.1)
	ωB97X-D		548	716	548 (ξ = 0)
	B3LYP	281	1308	618	515 (ξ = 0.6)
	DFT/50−50	304	183	775	606 (ξ = 0.1)
	ωB97X	599	709	718	709 (ξ = 0)
	LC-ωPBE	535	819	819	819 (ξ = 0)
	M06HF	681	898	818	898 (ξ = 0)
	HF	892	1761	991	1761 (ξ = 0)
M06HF	CAM-B3LYP		17	605	645 (ξ = 0.15)
	ωB97X-D		431	608	431 (ξ = 0)
	B3LYP	138	1614	618	609 (ξ = 0.7)
	DFT/50−50	257	170	775	641 (ξ = 0.2)
	ωB97X	788	560	611	560 (ξ = 0)
	LC-ωPBE	713	551	587	551 (ξ = 0)
	M06HF	656	725	725	725 (ξ = 0)
	HF	1130	1447	918	1447 (ξ = 0)

[a]The experimental electronic coupling is 430 cm^{-1} from ref 35. [b]The functionals used for the geometric optimization. [c]Different electronic structure methods used to calculate the electronic coupling.

and M06HF is suitable to describe the systems with fully localized charge.

In the TM model, we only use the mRTM to calculate the electronic couplings because the donor and acceptor fragments cannot be easily separated in the RTM model.[57] As discussed in the above section, the mRTM model involves the diabatic wave functions and Fock matrix in HF calculation and Kohn−Sham matrix in DFT calculation, allowing us easily to investigate the relationship between electronic coupling with Fock/Kohn−Sham matrix and wave functions. The Fock/Kohn−Sham matrices are obtained through the single-point calculations of the neutral systems at the optimized radical cationic geometries, while the wave functions are directly obtained from the HOMO and SOMO in the single-point calculations of the radical cationic systems or their combinations by eqs 7 and 8. Here, we choose the Fock/Kohn−Sham matrix and wave functions via two schemes to calculate the electronic couplings. In the first one (mRTM-1), the electronic structure methods for the calculations of Fock/Kohn−Sham matrix and wave functions are kept consistently. In the second scheme (mRTM-2), the wave functions are calculated from the methods used in the optimization of geometry, however, the Fock/Kohn−Sham matrices are obtained from many different methods, such as HF and B3LYP, listed in Tables 3 and 4. Obviously, the electronic couplings from mRTM-1 are very sensitive to the electronic structure methods and some electronic structure methods even predict the incorrect results because they can not describe the electronic states correctly. However, the mRTM-2 for the tested electronic structure methods predicts nearly the same electronic couplings, which are closer to the experimental ones. One thus expects that the accuracy of electronic couplings are much more sensitive to the wave functions rather than Fock/Kohn−Sham matrix. This property is significant because it allows us to suggest a generalized method to estimate the electronic coupling accurately yet simply. Based on this, we can first use suitable DFTs calculation to find the optimized geometry, and then use eqs 7 and 8 to construct the localized wave functions by adjusting ξ in order to get the good diabatic states (some examples are shown in Figures S2−S4). In the concrete implementation, we use the obtained localized wave functions to calculate the charge distributions in the redox centers, and the optimized ξ corresponds to the maximal charge distribution in one of the redox centers. Finally, we use the Fock/Kohn−Sham matrix of the neutral system and the constructed wave functions to calculate the electronic coupling. The functionals used in the latter two steps do not affect the values of electronic couplings too much. To demonstrate it, we calculate the electronic couplings with a variety of electronic structure methods and the results, labeled by mRTM-3, are also listed in Tables 3 and 4. The mRTM-3 is similar to mRTM-1 except that the localized wave functions are constructed by adjusting ξ with using of eqs 7 and 8. As expected, the predicted electronic couplings from different electronic structure methods are very close to one another.

Moreover, we have calculated the electronic couplings of $[D\text{-}ph\text{-}D]^{\bullet+}$ and $[D\text{-}(ph)_2\text{-}D]^{\bullet+}$ at the geometries from the charge localization (optimized geometry) to delocalization(transition state geometry), and the results are listed in the Table S8. It is found that the values of electronic coupling calculated at the different geometries have slight difference, manifesting that the non-Condon effect is not important in the present systems.

3.3. Dependence of Electronic Coupling on ω Value in LC-ωPBE. As discussed in the above section, the calculated electronic couplings from GMH are obviously sensitive to electronic structure methods and mRTM-3 is weakly dependent. But it is not clear how the electronic couplings depend on the long-range interaction term because the percent of HF exchange and the long-range correction in the functionals are mixed together and quite different. Therefore, in this section, we take LC-ωPBE as an example to investigate the influence of long-range term to the electronic coupling. The calculations are performed in the locally modified Q-Chem software package.

It is known that ω can be changed from 0 to 1 to adjust the length scale of long-range HF exchange. To investigate the effect of ω values on ionic geometries, we use LC-ωPBE with different ω to optimize $[D\text{-}ph\text{-}D]^{\bullet+}$ and $[D\text{-}(ph)_2\text{-}D]^{\bullet+}$ at the experimental twisting angles. Figure 4 shows the NPA charge distributions with respect to ω from the optimized geometry, where the charge is localized on the left sides of the systems. It is found that the charges in both of the systems are mostly distributed on the redox centers D^1 and D^2, and the total charges on the bridges are less than 20% for all ω values.

dx.doi.org/10.1021/jp308242s | J. Phys. Chem. B 2012, 116, 14126−14135

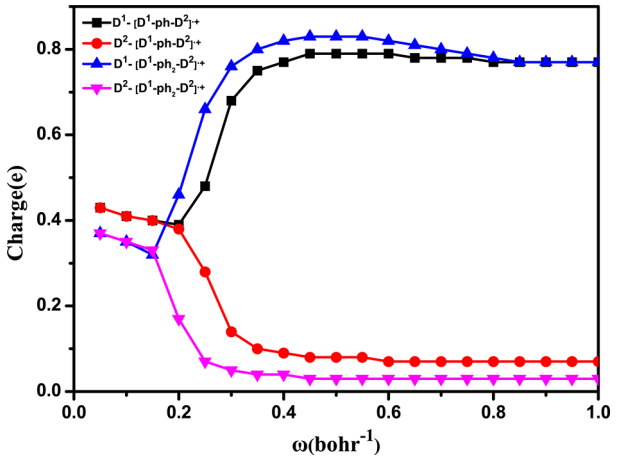

Figure 4. Dependence of the redox center charges on the ω in [D-ph-D]$^{\bullet+}$ and [D-(ph)$_2$-D]$^{\bullet+}$. D^1 and D^2 correspond to the left and right redox centers (as shown in Figure 1), respectively.

However, as the values of ω are smaller than 0.2, the charges on D^1 and D^2 are nearly equivalent. It means that the optimized systems are delocalized. When ω changes from 0.2 to 0.3, the charges rapidly become localized. Thereafter, the charges are almost constant with the increase of ω values. Although the charge distributions are reasonable for ω greater than 0.3, the optimized geometric parameters are explicitly different. Therefore, it seems hard to judge the correct ω value only from the charge distribution.

Thus, we have calculated the electronic couplings with GMH for the system [D-ph-D]$^{\bullet+}$ with use of different values of ω. The results are displayed in Figure 5. We find that the

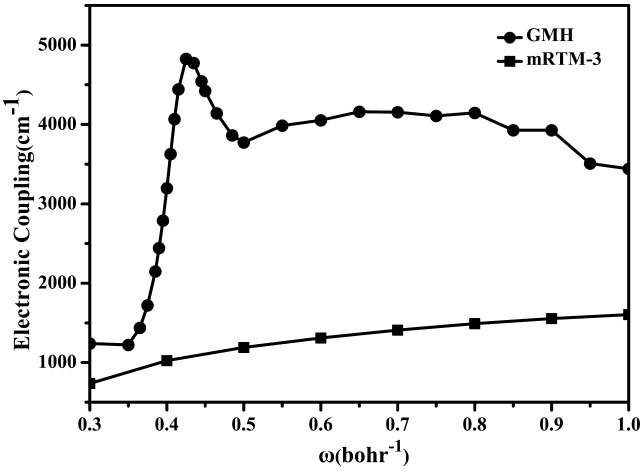

Figure 5. Electronic couplings obtained from the GMH and mRTM-3 with respect to ω for the [D-ph-D]$^{\bullet+}$ at its optimized geometry.

dependence of electronic coupling on ω is very similar to that of charge distributions, i.e., the electronic coupling is constant at small values (<0.35), and it dramatically increases in the range of about 0.35−0.50 and becomes constant again for larger ω. To deeply understand this property, we display the vertical excitation energies, transition dipole moments, and intrinsic dipole moment differences used in the GMH with respect to ω in Figure 6. It is seen that the vertical excitation energies always increase with the increase of the values of ω. It is consistent with the tendency of vertical excitation energy which becomes

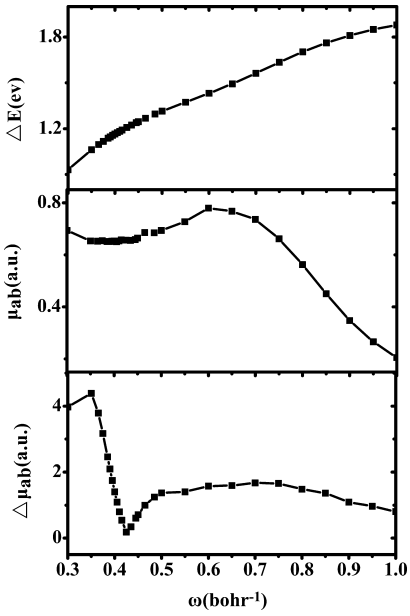

Figure 6. Vertical excitation energy, transition dipole moment, and difference of intrinsic dipole moments with respect to ω for [D-ph-D]$^{\bullet+}$.

large with the increasing of HF exchange percent in functionals. But the transition dipole moment μ_{ab} and the intrinsic dipole moment difference $\Delta\mu_{ab}$ are not monotonic along with the values of ω. Those jointed effects make the electronic couplings sensitive to ω values. Compared the calculated electronic couplings with the experimental one, it seems that the reasonable values of ω for the present systems should be within a very small interval, namely from 0.3 to 0.35 and the larger values of ω cause very large electronic couplings, which make it a challenge to correctly calculate the electronic coupling with GMH.

For the purpose of comparison, the mRTM-3 is used to calculate the electronic couplings with respect to the values of ω in LC-ωPBE. The results are also displayed in Figure 5. Compared to the results of GMH, the electronic couplings are indeed much less sensitive to the values of ω. Although the electronic couplings increase with the increase of the values of ω, their values only change from 700 cm^{-1} for the standard functional to 1600 cm^{-1} for the functional with 100% HF exchange, other than from 1000 to 3500 cm^{-1} in the GMH with the maximum value of 5000 cm^{-1}. It indicates the mRTM-3 is more stable and the electronic couplings are reasonable with a wide range of ω from 0.4 to 1.0. Thus, we expect that the proposed mRTM should be a robust technique to estimate the electronic couplings for intramolecular ET.

4. CONCLUDING REMARKS

The organic mixed-valence (MV) systems [D-(ph)$_n$-D]$^{\bullet+}$(D = 2,5-dimethoxy-4-methylphenyl, n = 0, 1, and 2) cover from classes II and III to the borderline class II/III. It thus becomes a challenge to theoretically optimize their structures and predict the electronic couplings for electron transfer. In the present work, we have adopted long-range corrected DFTs (LRC-DFTs) with CAM-B3LYP, ωB97X, ωB97X-D, and LC-ωPBE functionals, Hartree−Fock (HF) and the standard hybrid DFTs, such as B3LYP, DFT/50−50, and global hybrid meta-GGA functional M06HF to investigate their effects on the

dx.doi.org/10.1021/jp308242s | J. Phys. Chem. B 2012, 116, 14126−14135

structures and electronic couplings. The results show that for charge delocalized organic MV systems (i.e., $[D\text{-}D]^{\bullet+}$), CAM-B3LYP and ωB97X-D are suitable, however, M06HF and LC-ωPBE are more appropriate for bridged MV systems $[D\text{-}(ph)_2\text{-}D]^{\bullet+}$ and $[D\text{-}ph\text{-}D]^{\bullet+}$ having localized and almost localized charge distributions. In the electronic coupling calculations, we have employed the Koopmans' theorem (KT), the generalized Mulliken-Hush (GMH) method, and the reduced two-state model (RTM). For charge delocalized systems, all three models can predict the reasonable electronic couplings once the suitable electronic structure methods are used. For charge localized systems, however, the KT cannot directly used because the geometries for the curve crossing of two diabatic states are not easily determined. Although the GMH is a choice, the obtained electronic couplings are much sensitive to different electronic structure methods. We have thus proposed a modified RTM, named as mRTM, to calculate such intramolecular electronic couplings. In the proposed mRTM, the diabatic wave functions are constructed from the adiabatic ones, thus the method does not require to separate donor and acceptor fragments obviously, which is required in the RTM. This new model can predict the consistent electronic couplings with experimental ones. Furthermore, the electronic couplings from this model are insensitive to different electronic structure methods and they do not change too much with respect to the long-range correction of functionals. Therefore, the mRTM may be a good choice in the calculations of the intramolecular electronic couplings for the systems from class II to class III.

■ ASSOCIATED CONTENT

Supporting Information

Optimized geometric parameters with the different electronic structure methods for the redox centers of organic mixed-valence systems $[D\text{-}(ph)_n\text{-}D]^{\bullet+}$ (D = 2,5-dimethoxy-4-methylphenyl, n = 0, 1, and 2), expectation values of the total spin-squared operator, electronic couplings at different geometries obtained from a variety of R with the linear reaction coordinate and frontier molecular orbitals (MOs) in beta spin and their combinations. This material is available free of charge via the Internet at http://pubs.acs.org.

■ AUTHOR INFORMATION

Corresponding Author

*E-mail: yizhao@xmu.edu.cn.

Notes

The authors declare no competing financial interest.

■ ACKNOWLEDGMENTS

The authors thank Prof. WanZhen Liang for providing us the locally compiled Q-Chem software and her useful suggestions. The work is supported by the National Science Foundation of China (Grant Nos. 20833004, 21073146, and 21133007).

■ REFERENCES

(1) Demadis, K. D.; Hartshorn, C. M.; Meyer, T. J. *Chem. Rev.* **2001**, *101*, 2655−2685.
(2) Nelsen, S. F.; Pladziewicz, J. R. *Acc. Chem. Res.* **2002**, *35*, 247−254.
(3) Iyoda, M.; Hasegawa, M.; Miyake, Y. *Chem. Rev.* **2004**, *104*, 5085−5113.
(4) Benniston, A. C.; Harriman, A. *Chem. Soc. Rev.* **2006**, *35*, 169−179.
(5) Renz, R.; Theilacker, K.; Lambert, C.; Kaupp, M. *J. Am. Chem. Soc.* **2009**, *131*, 16292−16302.
(6) Hankache, J.; Wenger, O. S. *Chem. Rev.* **2011**, *111*, 5138−5178.
(7) Kaupp, M.; Renz, M.; Parthey, M.; Stolte, M.; Würthner, F. *Phys. Chem. Chem. Phys.* **2011**, *13*, 16973−16986.
(8) Völker, S.; Renz, M.; Kaupp, M.; Lambert, C. *Chem. Eur. J.* **2011**, *17*, 14147−14163.
(9) Heckmann, A.; Lambert, C. *Angew. Chem., Int. Ed.* **2012**, *51*, 326−392.
(10) Robin, M. B.; Day, P. *Adv. Inorg. Radiochem.* **1967**, *10*, 247−422.
(11) Jozefiak, T. H.; Miller, L. L. *J. Am. Chem. Soc.* **1987**, *109*, 6560−6561.
(12) Miller, L. L.; Liberko, C. A. *Chem. Mater.* **1990**, *2*, 339−340.
(13) Lin, C.-I.; Singh, P.; Ullman, E. F. *J. Am. Chem. Soc.* **1976**, *98*, 6713−6714.
(14) Hopf, F. R.; Mobius, D.; Whitten, D. G. *J. Am. Chem. Soc.* **1976**, *98*, 1586−1587.
(15) Nelsen, S. F. *J. Am. Chem. Soc.* **1996**, *118*, 2047−2058.
(16) Nelsen, S. F.; Ramm, M. T.; Wolff, J. J.; Powell, D. R. *J. Am. Chem. Soc.* **1997**, *119*, 6863−6872.
(17) Nelsen, S. F.; Weaver, M. N.; Telo, J. P.; Lucht, B. L.; Barlow, S. *J. Org. Chem.* **2005**, *70*, 9326−9333.
(18) Nelsen, S. F.; Li, G.-Q.; Schultz, K. P.; Tran, H. Q.; Guzei, I. A.; Evans, D. H. *J. Am. Chem. Soc.* **2008**, *130*, 11620−11622.
(19) Nelsen, S. F.; Schultz, K. P.; Telo, J. P. *J. Phys. Chem. A* **2008**, *112*, 12622−12628.
(20) Telo, J. P.; Nelsen, S. F.; Zhao, Y. *J. Phys. Chem. A* **2009**, *113*, 7730−7736.
(21) Jalilov, A. S.; Li, G.-Q.; Nelsen, S. F.; Guzei, I. A.; Wu, Q. *J. Am. Chem. Soc.* **2010**, *132*, 6176−6182.
(22) Rosspeintner, A.; Griesser, M.; Matsumoto, I.; Teki, Y.; Li, G.-Q.; Nelsen, S. F.; Gescheidt, G. *J. Phys. Chem. A* **2010**, *114*, 6487−6492.
(23) Qin, H. M.; Zhong, X. X.; Si, Y. B.; Zhang, W. W.; Zhao, Y. *J. Phys. Chem. A* **2011**, *115*, 3116−3121.
(24) Lambert, C.; Nöll, G.; Schelter, J. *Nat. Mater.* **2002**, *1*, 69−73.
(25) Lambert, C.; Nöll, G. *Synth. Met.* **2003**, *139*, 57−62.
(26) Lambert, C.; Risko, C.; Coropceanu, V.; Schelter, J.; Amthor, S.; Gruhn, N. E.; Durivage, J. C.; Brédas, J.-L. *J. Am. Chem. Soc.* **2005**, *127*, 8508−8516.
(27) Amthor, S.; Lambert, C. *J. Phys. Chem. A* **2006**, *110*, 1177−1189.
(28) Nöll, G.; Avola, M.; Lynch, M.; Daub, J. *J. Phys. Chem. C* **2007**, *111*, 3197−3204.
(29) Zhou, G.; Baumgarten, M.; Müllen, K. *J. Am. Chem. Soc.* **2007**, *129*, 12211−12221.
(30) Katting, D. R.; Mladenova, B.; Grampp, G.; Kaiser, C.; Heckmann, A.; Lambert, C. *J. Phys. Chem. C* **2009**, *113*, 2983−2995.
(31) Lancaster, K.; Odom, S. A.; Jones, S. C.; Thayumanavan, S.; Marder, S. R.; Brédas, J.-L.; Coropceanu, V.; Barlow, S. *J. Am. Chem. Soc.* **2009**, *131*, 1717−1723.
(32) Sun, D.-L.; Lindeman, S. V.; Rathore, R.; Kochi, J. K. *J. Chem. Soc. Perkins Trans. 2* **2001**, *9*, 1585−1594.
(33) Nelsen, S. F.; Li, G.-Q.; Konradsson, A. *Org. Lett.* **2001**, *3*, 1583−1586.
(34) Rosokha, S. V.; Sun, D.-L.; Kochi, J. K. *J. Phys. Chem. A* **2002**, *106*, 2283−2292.
(35) Lindeman, S. V.; Rosokha, S. V.; Sun, D.-L.; Kochi, J. K. *J. Am. Chem. Soc.* **2002**, *124*, 843−855.
(36) Sun, D.-L.; Rosokha, S. V.; Lindeman, S. V.; Kochi, J. K. *J. Am. Chem. Soc.* **2003**, *125*, 15950−15963.
(37) Barlow, S.; Risko, C.; Chung, S.-J.; Tucker, N. M.; Coropceanu, V.; Jones, S. C.; Levi, Z.; Brédas, J.-L.; Marder, S. R. *J. Am. Chem. Soc.* **2005**, *127*, 16900−16911.
(38) Barlow, S.; Risko, C.; Coropceanu, V.; Tucker, N. M.; Jones, S. C.; Levi, Z.; Khrustalev, V. N.; Antipin, M. Y.; Kinnibrugh, T. L.; Timofeeva, T.; et al. *Chem. Commun.* **2005**, *127*, 764−766.
(39) Lambert, C.; Nöll, G. *J. Am. Chem. Soc.* **1999**, *121*, 8434−8442.

(40) Brunschwig, B. S.; Creutz, C.; Sutin, N. *Chem. Soc. Rev.* **2002**, *31*, 168−184.
(41) Nishiumi, T.; Nomura, Y.; Chimoto, Y.; Higuchi, M.; Yamamoto, K. *J. Phys. Chem. B* **2004**, *108*, 7992−8000.
(42) Glover, S. D.; Kubiak, C. P. *J. Am. Chem. Soc.* **2011**, *133*, 8721−8731.
(43) Kurahashi, T.; Fujii, H. *J. Am. Chem. Soc.* **2011**, *133*, 8307−8316.
(44) Marcus, R. A.; Sutin, N. *Biochim. Biophys. Acta* **1985**, *811*, 265−322.
(45) Hänggi, P.; Talkner, P.; Borkovec, M. *Rev. Mod. Phys.* **1990**, *62*, 251−341.
(46) Hartmann, L.; Goychuk, I.; Hänggi, P. *J. Chem. Phys.* **2000**, *113*, 11159−11175.
(47) Barzykin, L.; Frantsuzov, P. A.; Seki, K.; Tachiya, M. *Adv. Chem. Phys.* **2002**, *123*, 511−616.
(48) Zhao, Y.; Liang, W. Z. *Chem. Soc. Rev.* **2012**, *41*, 1075−1087.
(49) Nelsen, S. F.; Blackstock, S. C.; Kim, Y. *J. Am. Chem. Soc.* **1987**, *109*, 677−682.
(50) Nelen, S. F.; Adamus, J.; Wolff, J. J. *J. Am. Chem. Soc.* **1994**, *116*, 1589−1590.
(51) Nelsen, S. F.; Ismagilov, R. F.; Trieber, D. A. *Science* **1997**, *278*, 846−849.
(52) Zhang, W. W.; Zhu, W. J.; Zhao, Y. *J. Phys. Chem. B* **2008**, *112*, 11079−11086.
(53) Farazdel, A.; Dupuis, M.; Clementi, E.; Avitam, A. *J. Am. Chem. Soc.* **1990**, *112*, 4206−4214.
(54) Nelsen, S. F.; Weaver, M. N.; Zink, J. I.; Telo, J. P. *J. Am. Chem. Soc.* **2005**, *127*, 10611−10622.
(55) Chen, H.-C.; Hus, C.-P. *J. Phys. Chem. A* **2005**, *109*, 11989−11995.
(56) Krylov, A. I. *Chem. Phys. Lett.* **2001**, *338*, 375−384.
(57) Valeev, E. F.; Coropceanu, V.; da Silva Filho, D. A.; Salman, S.; Brédas, J.-L. *J. Am. Chem. Soc.* **2006**, *128*, 9882−9886.
(58) Lambert, C.; Nöll, G.; Hampel, F. *J. Phys. Chem. A* **2001**, *105*, 7751−7758.
(59) Coropceanu, V.; Malagoli, M.; André, J. M.; Brédas, J.-L. *J. Chem. Phys.* **2001**, *115*, 10409−10416.
(60) Nelsen, S. F.; Blomgren, F. *J. Org. Chem.* **2001**, *66*, 6551−6559.
(61) Coropceanu, V.; Malagoli, M.; André, J. M.; Brédas, J.-L. *J. Am. Chem. Soc.* **2002**, *124*, 10519−10530.
(62) Nelsen, S. F.; Weaver, M. N.; Konradsson, A. E.; Telo, J. P.; Clark, T. *J. Am. Chem. Soc.* **2004**, *126*, 15431−15438.
(63) Coropceanu, V.; Gruhn, N.; Barlow, S.; Lambert, C.; Durivage, J. C.; Bill, T. G.; Nöll, G.; Marder, S. R.; Brédas, J.-L. *J. Am. Chem. Soc.* **2004**, *126*, 2727−2731.
(64) Lambert, C.; Amthor, S.; Schelter, J. *J. Phys. Chem. A* **2004**, *108*, 6474−6486.
(65) Risko, C.; Coropceanu, V.; Barlow, S.; Geskin, V.; Schmidt, K.; Gruhn, N. E.; Marder, S. R.; Brédas, J.-L. *J. Phys. Chem. C* **2008**, *112*, 7959−7967.
(66) Nelsen, S. F.; Schultz, K. P. *J. Phys. Chem. A* **2009**, *113*, 5324−5332.
(67) Heckmann, A.; Lambert, C. *J. Am. Chem. Soc.* **2007**, *129*, 5515−5527.
(68) Yanai, T.; Tew, D. P.; Handy, N. C. *Chem. Phys. Lett.* **2004**, *393*, 51−57.
(69) Tawada, Y.; Tsuneda, T.; Yanagisawa, S.; Yanai, T.; Hirao, K. *J. Chem. Phys.* **2004**, *120*, 8425−8433.
(70) Zhao, Y.; Truhlar, D. G. *J. Phys. Chem. A* **2006**, *110*, 5121−5129.
(71) Zhao, Y.; Truhlar, D. G. *J. Phys. Chem. A* **2006**, *49*, 13126−13130.
(72) Vydrov, O. A.; Heyd, J.; Krukau, A. V.; Scuseria, G. E. *J. Chem. Phys.* **2006**, *125*, 074106.
(73) Vydrov, O. A.; Scuseria, G. E. *J. Chem. Phys.* **2006**, *125*, 234109.
(74) Vydrov, O. A.; Scuseria, G. E.; Perdew, J. P. *J. Chem. Phys.* **2007**, *126*, 154109.
(75) Chai, J.-D.; Head-Gordon, M. *Phys. Chem. Chem. Phys.* **2008**, *10*, 6615−6620.
(76) Olah, G. A.; Reddy, V. P.; Rasul, G.; Prakash, G. K. S. *J. Am. Chem. Soc.* **1999**, *121*, 9994−9998.
(77) Cee, V. J.; Cramer, C. J.; Evans, D. A. *J. Am. Chem. Soc.* **2006**, *128*, 2920−2930.
(78) Pan, F.; Gao, F.; Liang, W. Z.; Zhao, Y. *J. Phys. Chem. B* **2009**, *113*, 14581−14587.
(79) Song, J.; Gao, F.; Shi, B.; Liang, W. Z. *Phys. Chem. Chem. Phys.* **2010**, *12*, 13070−13075.
(80) Song, J.; Gao, F.; Liang, W. Z. *Comput. Theor. Chem.* **2011**, *965*, 53−59.
(81) You, Z.-Q.; Shao, Y.; Hus, C.-P. *Chem. Phys. Lett.* **2004**, *390*, 116−123.
(82) Coropceanu, V.; Cornil, J.; da Silva Filho, D. A.; Olivier, Y.; Silbey, R.; Brédas, J.-L. *Chem. Rev.* **2007**, *107*, 926−952.
(83) Hus, C.-P. *Acc. Chem. Res.* **2009**, *42*, 509−518.
(84) Jordan, K. D.; Paddon-Row, M. N. *Chem. Rev.* **1992**, *92*, 395−410.
(85) Nelsen, S. F.; Weaver, M. N.; Yamazaki, D.; Komatsu, K.; Rathore, R.; Bally, T. *J. Phys. Chem. A* **2007**, *111*, 1667−1676.
(86) You, Z.-Q.; Hsu, C.-P.; Fleming, G. R. *J. Chem. Phys.* **2006**, *124*, 044506.
(87) Cave, R. J.; Newton, M. D. *Chem. Phys. Lett.* **1996**, *249*, 15−19.
(88) Cave, R. J.; Newton, M. D. *J. Chem. Phys.* **1997**, *106*, 9213−9226.
(89) He, R. X.; Duan, X. H.; Li, X. Y. *J. Phys. Chem. A* **2005**, *109*, 4154−4161.
(90) Kestner, N. R.; Logan, J.; Jortner, J. *J. Phys. Chem.* **1974**, *78*, 2148−2166.
(91) Brunschwig, B. S.; Marshall, J. L.; Newton, M. D.; Sutin, N. *J. Am. Chem. Soc.* **1980**, *102*, 5798−5809.
(92) Larsson, S. *J. Am. Chem. Soc.* **1981**, *103*, 4034−4040.
(93) Logan, T.; Newton, M. D. *J. Chem. Phys.* **1983**, *78*, 4086−4091.
(94) Larsson, S. *J. Chem. Soc., Faraday Trans. 2* **1983**, *79*, 1375−1388.
(95) Newton, M. D.; Sutin, N. *Auu. Rev. Phys. Chem.* **1984**, *35*, 437−480.
(96) Rodriguez-Monge, L.; Larsson, S. *Int. J. Quantum Chem.* **1997**, *61*, 847−857.
(97) Newton, M. D. *J. Phys. Chem.* **1988**, *92*, 3049−3056.
(98) Farazdel, A.; Dupuis, M. *J. Comput. Chem.* **1991**, *12*, 276−282.
(99) Becke, A. D. *J. Chem. Phys.* **1993**, *98*, 5648−5652.
(100) Stephens, P. J.; Devlin, F. J.; Chabalowski, C. F.; Frisch, M. J. *J. Chem. Phys.* **1994**, *98*, 11623−11627.
(101) Shao, Y.; Head-Gordon, M.; Krylov, A. I. *J. Chem. Phys.* **2002**, *118*, 4807−4818.
(102) Chai, J.-D.; Head-Gordon, M. *J. Chem. Phys.* **2008**, *128*, 084106.
(103) Rohrdanz, M. A.; Martins, K. M.; Herbert, J. M. *J. Chem. Phys.* **2009**, *130*, 054112.
(104) Song, J.; Liang, W. Z.; Zhao, Y.; Yang, J. L. *Appl. Phys. Lett.* **2006**, *89*, 071917.
(105) Chai, J.-D.; Head-gordon, M. *Chem. Phys. Lett.* **2008**, *467*, 176−178.
(106) Ma, H. L.; Gao, F.; Liang, W. Z. *J. Phys. Chem. C* **2012**, *116*, 1755−1763.
(107) Frisch, M. J.; et al. *Gaussian 09*, revision A.02; Gaussian Inc.: Wallingford, CT, 2009.
(108) Kong, J.; White, C. A.; Krylov, A. I.; Sherrill, C. D.; Adamson, R. D.; Furlani, T. R.; Lee, M. S.; Lee, A. M.; Gwaliney, S. R.; Adams, T. R.; et al. *Phys. Chem. Chem. Phys.* **2006**, *8*, 3172−3191.